Magnetic Heuslers for applications

Michael Nicklas[#], Niels-O. Born, Claudia Felser, Robert Küchler, Sergiy A. Medvedev, Kamal Mydeen, Ajaya K. Nayak, Pavel Naumov, Catalina Salazar Mejía, Ulrich Schwarz, C. Wang

Heusler alloys display diverse functional properties which stem from magnetoelastic couplings, such as the shape memory, magnetic superelastic, magnetocaloric, and barocaloric effects. These properties make them highly attractive for the use as sensors, actuators, energy harvesters, and in magnetic cooling devices. In our studies we focus on the investigation of the basic physical mechanisms behind the strong magnetoelastic couplings in the Ni-Mn-*X* (*X* = Mn, Ga, Sb) families. We employ different techniques, such as resonant-ultrasound spectroscopy, magnetostriction, and X-ray diffraction, and correlate their results with data from detailed magnetic investigations.

Magnetic shape-memory Heusler alloys have attracted a huge amount of attention in the material science community in recent years. The diverse potential applications of their non-magnetic counterparts are extended in the magnetic shape-memory alloys since the magnetic field can be used to control the shape-memory effect. Typical applications include sensors, actuators, energy harvesters, and magnetic cooling devices.

In this collaboration of the Physics of Quantum Materials, the Chemical Metals Science and the Solid state Chemistry departments, we focus on exploring the basic physical phenomena in magnetic Heusler shape-memory alloys. Our results have led to a deeper understanding of the coupling of magnetic and structural degrees of freedom. To gain these new insights we combined different physical probes, such as magnetization, resonant ultrasound spectroscopy (RUS), X-ray diffraction and magnetostriction/thermal contraction. In addition, we tuned the materials by application of hydrostatic and uniaxial pressure which provides further insights for the directions to go in designing materials with specific properties.

Previously, we investigated the correlation between magnetism and structure on different time scales and its consequences on the hysteresis and reversibility / irreversibility in Heusler alloys for magnetocaloric applications [1, 2]. We looked for the correlation between the crystal structure and reversibility of the phase transitions, response time and relaxation effects and the coupling between different degrees of freedom on the example of $Ni_{50}Mn_{35}In_{15}$ [1, 2]. For that study we successfully developed and employed a technique for magnetocaloric measurements in pulsed magnetic fields [2]. To obtain further insights on the coupling of magnetic and structural degrees of freedom magnetic in shape-memory Heusler alloys we continued our study on $Ni_{50}Mn_{35}In_{15}$ by employing RUS techniques and by using external hydrostatic pressure in combination with magnetization and X-ray diffraction. Furthermore, we extended our scope on related materials, such as the Ni-Mn-Ga and the Ni-Mn-Sb families of Heusler alloys.

Strain and order-parameter coupling

Resonant ultrasound spectroscopy is a powerful technique to elucidate strain coupling phenomena associated with structural and magnetic properties in shape memory Heusler alloys, whose understanding is essential for the design of new compounds with optimized properties. We carried out the RUS experiments in close collaboration with the Group of M. A. Carpenter at the University of Cambridge.

Upon decreasing temperature $Ni_{50}Mn_{35}In_{15}$ exhibits a ferromagnetic transition within the austenitic phase followed by the magnetostructural martensitic

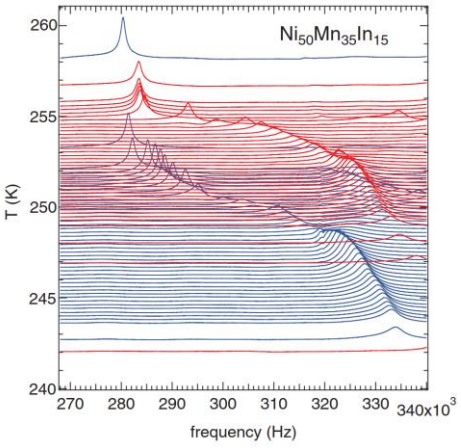

Fig.-1: RUS spectra taken at different temperatures through the martensitic transition. The ordinate is amplitude in volts, but each spectrum has been offset in proportion to the temperature at which it was collected and the axis is labeled as temperature. Blue traces are spectra collected during cooling and red traces are spectra collected during heating (taken from Ref. 3).

transformation from the austenitic to the martensitic phase. Further changes of the magnetic structure take place at lower temperatures inside the martensitic phase.

Figure 1 displays the RUS spectra taken on $Ni_{50}Mn_{35}In_{15}$ upon cooling (blue) and heating (red) [3]. The spectra show characteristic resonance peaks. The analysis of the frequency f^2 and width Δf provide information on the shear modulus and acoustic attenuation in $Ni_{50}Mn_{35}In_{15}$. In Fig. 2, we clearly recognize the ferromagnetic ordering in the austenitic phase at $T_C{}^A$ and the kink at T_B related to the formation of a spin-glass-like magnetic state. However, the most prominent feature is the pronounce jump in $f^2(T)$ at the martensitic transformation at $T_{M(A)}$.

Our results indicate that the dominant changes in the shear modulus are connected with the large shear strains associated with the martensitic transition. A strong stiffening of the lattice is accompanied by a marked increase in the acoustic loss. The large damping in the martensite phase in comparison with the austenite phase points at the presence and mobility of twin boundaries, while the small feature at the ferromagnetic transition reflects the weak coupling of the ferromagnetic order parameter with shear strain [3].

In the model system $Ni_{50+x}Mn_{25-x}Ga_{25}$, we characterized the strain coupling phenomena associated with structural and magnetic properties for four different representative scenarios as indicated in the schematic phase diagram in presented in Fig. 3: $T_C > T_{PM} > T_M$, $T_C > T_M$ without premartensitic transition, $T_C \approx T_M$, and $T_C < T_M$ (here T_{PM} refers to the premartensitic transition) [4]. We obtained a coherent picture of the consequences of strain coupling effects associated with the particular combination of instabilities that is commonly observed in Heusler alloys. The coupling of the three order parameters, namely the electronic Q_E, ferromagnetic Q_M, and structural Q_S order parameters, can account for the topology of the phase diagram as displayed in Fig. 3, as well as for the particular structure types which are observed in Ni-Mn-Ga alloys. The acoustic losses, on the other hand, can be attributed to critical slowing down at the premartensite transition, to the mobility of interfaces between coexisting phases at the martensitic transition, and to mobility of the twin boundaries.

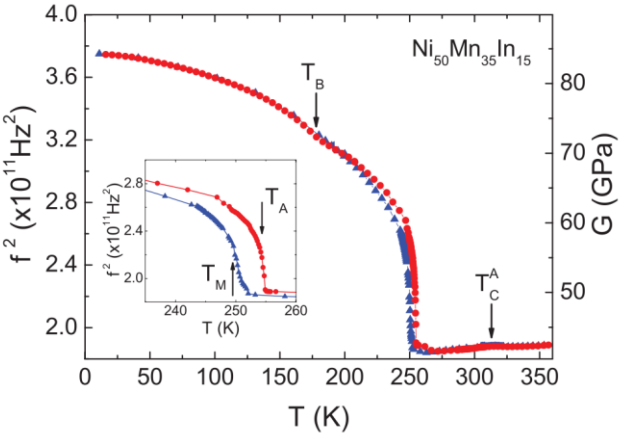

Fig.-2: Temperature dependence f^2 (left axis) and variation of the absolute value of the shear modulus obtained by scaling $f^2(T)$ to literature data at room temperature (right axis) for the series $Ni_{50+x}Mn_{25-x}Ga_{25}$ (taken from Ref. 3).

Tuning magnetism in $Ni_{50}Mn_{35}In_{15}$ by hydrostatic pressure

The application of pressure is expected to have a strong influence on the magnetic properties in shape-memory alloys due to the strong coupling of the structural transition to magnetic degrees of freedom. By complementary magnetization and X-ray diffraction experiments performed at hydrostatic pressures up to 5 GPa using diamond anvil cells, we established a combined structural and magnetic temperature-pressure (T-p) phase diagram of $Ni_{50}Mn_{35}In_{15}$ [5]. The phase diagrams for cooling and heating protocols are depicted in Fig. 4. The main finding is a suppression of the ferromagnetic order by hydrostatic pressure, while the transition temperature $T_C{}^A$ is almost unaffected. At the same time the mar-tensitic phase is stabilized. The martensitic transition shifts to higher temperatures and

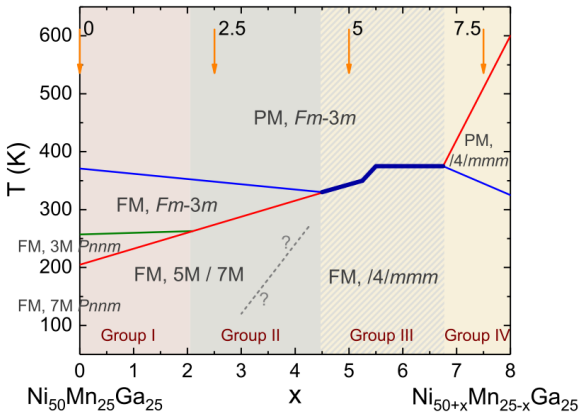

Fig.-3: Schematic phase diagram for the Ni-rich end of the system $Ni_{50+x}Mn_{25-x}Ga_{25}$. Ferromagnetic structures become stable below the blue line (T_C) and martensitic structures become stable below the red line (T_M). The green line is T_{PM} , which marks the transition from the ferromagnetic austenite structure to the premartensite structure (taken from Ref. 4).

suppresses the ferromagnetic austenitic phase. The magnetization does not show any indication of ferromagnetic ordering above 3 GPa, where the martensitic-transition temperature approaches the Curie temperature in the austenite. We notice that the mixed-phase region of austenitic and martensitic phases and its relation with $T_C{}^A$ determines the magnetic properties of the material. This confirms the expected strong coupling of the magnetic and structural properties at the martensitic transition in Ni-Mn based Heusler compounds.

Uniaxial-stress-tuned large magnetic shape-memory effect in Ni-Co-Mn-Sb

In Ni-Co-Mn-Sb our combined strain and magnetization measurements provide evidence for a strong magneto-structural coupling [6]. In order to determine the magnetostriction, respectively, thermal contraction, we used a miniature dilatometer developed at the MPI-CPfS [7]. A modified version of the miniature dilatometer was deployed to apply a uniaxial stress on the sample during the experiment [8].

In $Ni_{45}Co_5Mn_{38}Sb_{12}$ and $Ni_{44}Co_6Mn_{38}Sb_{12}$ we found length changes of more than 1% at the martensitic transformation between a ferromagnetic, austenitic phase at high temperatures and a weakly magnetic, low-symmetry martensitic phase at lower temperatures. In the vicinity of the temperature controlled martensitic transformation, either a one- or two-way magnetic shape-memory effect can be generated by the magnetic field depending on small variations in temperature (see Fig. 5). We note that the length change is mostly reversible except a small initial offset in the virgin curve.

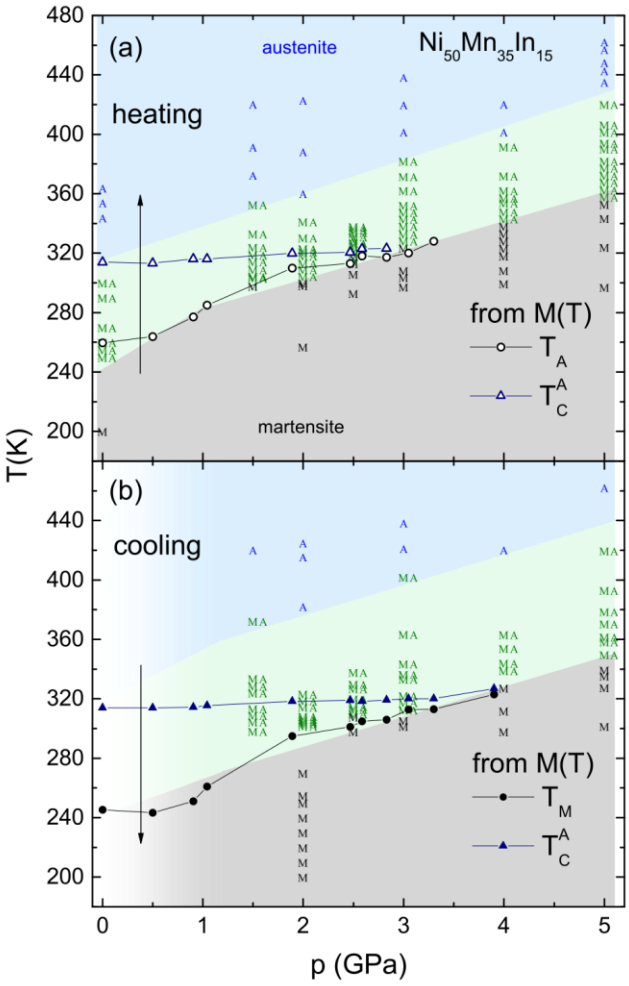

Fig.-4: T–p phase diagram of $Ni_{50}Mn_{35}In_{15}$ determined on (a) heating and (b) cooling cycles by XRD and magnetization experiments. The austenitic phase is labeled by the letter A (blue), the mixed martensitic and austenitic phases by MA (green), and the martensitic phase by M (black) (taken from Ref. 5).

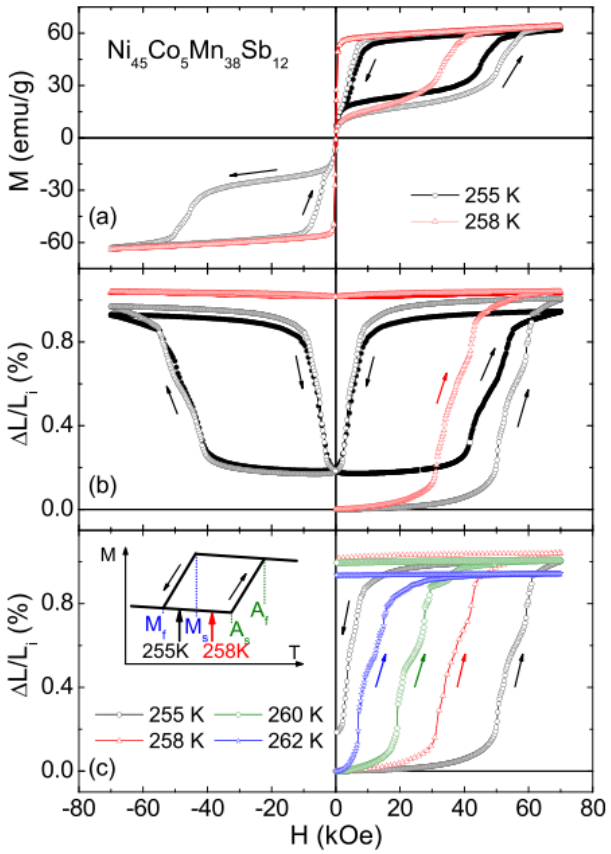

Fig.-5: Magnetization M(H) and strain $\Delta L(H)/L_i$ of $Ni_{45}Co_5Mn_{38}Sb_{12}$ recorded at two different constant temperatures. L_i is the initial length of the sample before the application of the magnetic field. (a) and (b) Hysteresis loops of M and $\Delta L(H)/L_i$. Open and closed symbols indicate the first and second cycles, respectively. (c) $\Delta L(H)/L_i$ at different temperatures in the vicinity of the martensitic transition as illustrated in the inset (taken from Ref. 6).

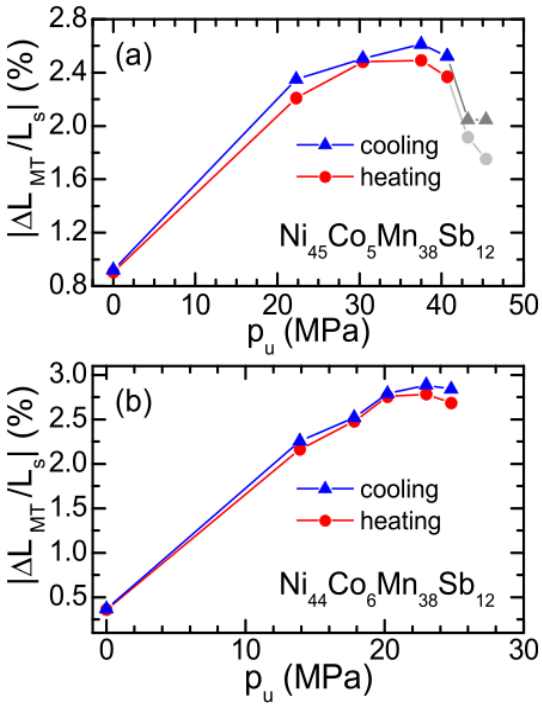

Fig.-6: Relative length change of the sample at the martensitic transition $|\Delta L_{MT}/L_s|$ as a function of the applied uniaxial stress p_u (taken from Ref. 6).

Figure 6 displays the relative length change $|\Delta L_{MT}/L_s|$ at the martensitic transformation as function of the uniaxial stress p_u. The application of a moderate uniaxial stress led first to a substantial increase in $|\Delta L_{MT}/L_s|$ at the temperature-induced martensitic transition followed by a saturation at $|\Delta L_{MT}/L_s|$ of about 3%. The saturation behavior points at a stabilization of a single martensitic variant.

The observation that slight differences in temperature changes drastically the response of the material indicates the large potential shape-memory Heusler alloys have for prospective applications as actuators, sensors, and mechanical switches.

Conclusion

Our studies on the Ni-Mn-*X* (*X* = Mn, Ga, Sb) based shape-memory Heusler alloys exemplify the strong coupling of structural and magnetic degrees of freedom and the importance for their functional properties in these class of materials. Only a combination of complementary techniques, as we used in our investigations, is capable of providing these type of fundamental insights.

External Cooperation Partners

M. Hanfland (ESRF Grenoble, France); M. A. Carpenter, J. A. Schiemer (Department of Earth Sciences, University of Cambridge, United Kingdom)

References

[1]* *Pulsed high-magnetic-field experiments: New insights into the magnetocaloric effect in Ni-Mn-In Heusler alloys, C. Salazar Mejía, M. Ghorbani-Zavareh, A. K. Nayak, Y. Skourski, J. Wosnitza, C. Felser and M. Nicklas, J. Appl. Phys.* ***117*** *(2015) 17E710, DOI:10.1063/1.4916556.*

[2]* *Direct measurements of the magnetocaloric effect in pulsed magnetic fields: The example of the Heusler alloy $Ni_{50}Mn_{35}In_{15}$, M. Ghorbani Zavareh, C. Salazar Mejía, A. K. Nayak, Y. Skourski, J. Wosnitza, C. Felser and M. Nicklas, Appl. Phys. Lett.* ***106*** *(2015) 071904, DOI:10.1063/1.4913446.*

[3]* *Strain behavior and lattice dynamics in $Ni_{50}Mn_{35}In_{15}$. C. Salazar Mejía, A. K. Nayak, J. A. Schiemer, C. Felser, M. Nicklas and M. A. Carpenter, J. Phys.: Condens. Matter* ***27*** *(2015) 415402, DOI:10.1088/0953-8984/27/41/415402.*

[4]* *Strain and order-parameter coupling in Ni-Mn-Ga Heusler alloys from resonant ultrasound spectroscopy, C. Salazar Mejía, N.-O. Born, J. A. Schiemer, C. Felser, M. A. Carpenter and M. Nicklas, Phys. Rev. B* ***97*** *(2018) 094410, DOI:10.1103/PhysRevB.97.094410.*

[5]* *Suppression of the ferromagnetic order in the Heusler alloy $Ni_{50}Mn_{35}In_{15}$ by hydrostatic pressure, C. Salazar Mejía, K. Mydeen, P. Naumov, S. A. Medvedev, C. Wang, M. Hanfland, A. K. Nayak, U. Schwarz, C. Felser and M. Nicklas, Appl. Phys. Lett.* ***108*** *(2016) 261903, DOI:10.1063/1.4954838.*

[6]* *Uniaxial-stress tuned large magnetic-shape-memory effect in Ni-Co-Mn-Sb Heusler alloys, C. Salazar Mejía, R. Küchler, A. K. Nayak, C. Felser and M. Nicklas, Appl. Phys. Lett.* ***110*** *(2017) 071901, DOI:10.1063/1.4976212.*

[7]* *A compact and miniaturized high resolution capacitance dilatometer for measuring thermal expansion and magnetostriction, R. Küchler, T. Bauer, M. Brando and F. Steglich, Rev. Sci. Instr.* ***83*** *(2012) 095102, DOI: 10.1063/1.4748864.*

[8]* *A uniaxial stress capacitive dilatometer for high-resolution thermal expansion and magnetostriction under multiextreme conditions, R. Küchler, C. Stingl and P. Gegenwart, Rev. Sci. Instr.* ***87*** *(2016) 073903, DOI: 10.1063/1.4958957.*

nicklas@cpfs.mpg.de